Journal of Engineering Science and Technology
Vol. 16, No. 2 (2021) 1213 - 1231

ASSESSMENT OF ADSORBENT FOR REMOVING LEAD (Pb) ION IN AN INDUSTRIAL-SCALED PACKED BED COLUMN

MOHD HARDYIANTO VAI BAHRUN[1], ZYKAMILIA KAMIN[2,*], S. M. ANISUZZAMAN[1], AWANG BONO[1]

[1]Chemical Engineering Programme, Faculty of Engineering, 88400 Universiti Malaysia Sabah, Malaysia
[2]Oil and Gas Engineering Programme, Faculty of Engineering, 88400 Universiti Malaysia Sabah, Malaysia
*Corresponding Author: zykamilia@ums.edu.my

Abstract

Adsorption is becoming a prominent method to remove heavy metal ions from wastewater due to its ability to remove pollutant at extremely low concentration. In batch experimental studies, activated alumina shows a good adsorption capacity towards lead Pb(II). Subsequently, this study was conducted to simulate the performance of activated alumina in a packed bed column to remove Pb(II) presents in wastewaters, using Aspen Adsorption® based on data from batch experiments. A plug flow mathematical model, with a linear driving force (LDF) approximation was used for the simulation. A dynamic column performance was evaluated systematically at various parameters. The simulated results show that a decrease in the inlet flowrate and inlet concentration, and an increase in both bed height and bed diameter enhance the Pb(II) adsorption by the column by delaying the breakthrough time. In addition, a real activated alumina industrial packed bed column plant, namely Plant D was employed as a case study for a scale-up analysis. A sensitivity analysis of three model parameters revealed that the activated alumina column was very sensitive towards the changes in isotherm model and bed porosity, and insignificant to the changes in LDF mass transfer coefficient. The size of a packed bed column was taken to be 1.459 m and 0.6090 m, for height and diameter, respectively. The corresponding operation time was 28 days at inlet flowrate and inlet concentration of 6.31×10^{-4} m^3/s and 0.1 mg/L, respectively. These figures seem to be practical and manageable for industrial wastewater treatment plant.

Keywords: Breakthrough curve, Dynamic simulation, Heavy metal, Mass transfer coefficient, Scale-up.

1. Introduction

Heavy metals in water bodies could be concentrated in the living tissues of organisms [1-3] due to the increase in industrial activities such as battery manufacturing, mining, smelting, refining and soldering [4-6], therefore intensified environmental pollution [7]. Lead, for example, cause malfunctioning of human central nervous system, immune system, excretory system and cardiovascular system [8]. Moreover, the concentration of heavy metals in industrial effluent usually exceeds the threshold limit set by governing bodies, thus need to be reduced within this limit before being discharged. Several processes are being developed for this issue, such as membrane filtration, chemical precipitation and ion-exchange [9-12].

Adsorption is an economic–process to separate heavy metal from aqueous solution, since it is a simple, non-energy intensive and highly efficient operation without toxic sludge generation [13-17]. Many adsorbents are being developed for organic or inorganic environment, having comprehensive isotherm data [18-22]. A study by Naiya et al. [22] shows that activated alumina has a good adsorption capacity towards heavy metals (Pb and Cd) in aqueous solution in batch experiments. Activated alumina has a highly porous surface area, good mechanical strength and has both acidic and basic characters [22, 23], as well as a low toxicity and less sludge involvement [3, 24] to make a metal ion adsorbent. However, experimental approaches are costly and time-consuming. It limits the evaluation of operating variables needed to design a packed bed column. In some cases, it is difficult to hold certain variables constant [25]. From the isotherm data, a feasibility study can be further investigated to prove their practicability over a larger scale for application such as in wastewater treatment.

A packed bed adsorption column is a device filled with adsorbent, in which a solution containing pollutants to be removed is passed through the adsorbent bed and get attached onto the surface of the adsorbent [26, 27]. Continuous packed bed adsorption column is preferred for an industrial wastewater treatment processes due to its ability to handle large volumes [28, 29] and simple operation [30]. It also provides information on breakthrough and exhaustion times, which are important to evaluate the feasibility of adsorbents [29, 31]. A packed bed column operates until the adsorbent bed is saturated with the pollutants and lose its adsorption capacity [32].

From the packed bed column experiment, breakthrough curve can be generated which is then used to design adsorption column, and provide information on the concentration of a dynamic response of a system with a function of time elapsed [33]. Numerous authors have investigated the adsorption of heavy metals in a small scale continuous packed bed column via experimental works [34-37], but, few studies reported on the attempt to model and simulate the system for future transition from laboratory to industrial application [38, 39]. Thus, it is necessary to establish a mathematical model of a small-scale packed bed column for future use in designing for larger industrial scale application. A few mathematical models have been developed for packed bed adsorption columns, both analytically and numerically. Examples of analytical models that is widely adapted in the modelling adsorption column are Thomas model, Yoon-Nelson model and Bohart-Adams model [40]. However, the analytical models have drawback of not being well correlated with the experimental data [41], especially for asymmetrical breakthrough curves. Numerical model, on the other hand, has the advantages over the analytical model, for instance, it represents the system more general and accurate and is

mathematically rigid, despite of its complicated numerical solutions and long computational time [40, 41].

Therefore, in this present work, simulation of packed bed adsorption of Pb(II) ion onto activated alumina was carried out using Aspen Adsorption V7.3 simulator tool to solve sets of equations of the model. Factors affecting the dynamic column performance were investigated, including the effect of inlet flowrate, inlet concentration, bed height and bed diameter. Then, the system was upscale with reference to industrial scale to verify the feasibility of the adsorbent to be used for treating Pb(II)-containing wastewater in aspects of practicability and manageability.

2. Methodology

2.1. Data extraction

This study was based on the data by Naiya et al. [22] and used for a case study for this simulation. The dynamic adsorption simulation was conducted by using Aspen Adsorption® V7.3. The required data for the simulation on the adsorbent properties and adsorption isotherm are presented in Tables 1 and 2, respectively.

Table 1. Characteristics of activated alumina [22].

Parameter	Value
BET surface area, m^2/g	126
Effective particle diameter, μm	291.45
Bulk density, kg/m^3	810

Table 2. Langmuir and Freundlich isotherm parameter [22].

Langmuir isotherm	Q_{max} (mg/g)	83.33
	K_L (L/mg)	0.0515
	R^2	0.974
Freundlich isotherm	K_F ({mg/g}/{mg/L}$^{1/n}$)	3.82
	1/n	1.44
	R^2	0.994

2.2. Mathematical model framework

2.2.1. Continuity equation around a packed bed column

Consider a control volume with a height Δz and a cross-sectional area of the column A. A fluid stream containing component i to be adsorbed flows through the beds with void ε. Then, the volume of solid V_s is the control volume,

$$V_s = (1 - \varepsilon)A\Delta z \tag{1}$$

By applying the mass balance of the component i in the fluid phase of the inlet term, outlet, and accumulation of the component in the control volume

$$(u_0\varepsilon C_i)_z - (u_0\varepsilon C_i)_{z+\Delta z} - \left(\varepsilon D_{Li}\frac{\partial C_i}{\partial z}\right)_z + \left(\varepsilon D_{Li}\frac{\partial C_i}{\partial z}\right)_{z+\Delta z} - \rho_s\Delta z\frac{\partial Q_i}{\partial t} = \varepsilon\Delta z\frac{\partial C_i}{\partial t} \tag{2}$$

where D_{Li} is the axial dispersion coefficient of component i (m^2/s), ρ_s is the bed column density (kg/m^3), u_0 is the interstitial velocity (m/s), z is the bed axial position (m), t is the process time (s), C_i is the aqueous-phase concentration of component i (mg/L) and Q_i is the solid-phase loading of component i (mg/g).

Dividing Eq. (2) by $\varepsilon A \Delta z$ and applying the limit $\Delta z \rightarrow 0$, definition of derivatives and negligible axial dispersion term assumption yields Eq. (3).

$$u_o \varepsilon \frac{\partial C_i}{\partial z} + \varepsilon \frac{\partial C_i}{\partial t} + \rho_s \frac{\partial Q_i}{\partial t} = 0 \tag{3}$$

2.2.2. Simplified kinetic models

The kinetic mass transfer coefficient was adequately assumed to follow LDF approximation as popularized by Glueckauf [42], in which the mass transfer driving force for a component *i* is a linear function of the solid phase loading [43]. The LDF approximation is often used in the analysis of adsorption process due to its mathematically-view simple without jeopardizing the accuracy [44]. In this work, two independent mass transfer diffusion were lumped by linear addition into the LDF mass transfer coefficient [45].

$$\frac{\partial Q_i}{\partial t} = MTC\left(Q_i^{*} - Q_i\right) \tag{4}$$

$$\frac{1}{MTC} = \frac{R_p}{3k_f} + \frac{R_p^{2}}{15D_s} \tag{5}$$

where Q_i^* is solid-phase loading of component *i* at interface (mg/g) and *MTC* is the LDF mass transfer coefficient (1/s). For the range of $0.001 < Re_p < 5.8$ found in this work, the film mass transfer diffusion, k_f (m/s) can be calculated by using Sherwood (Sh) correlation as developed by [46].

$$Sh = \frac{2R_p k_f}{D_m} = 2.0 + 1.58Re^{0.4}Sc^{\frac{1}{3}} \tag{6}$$

where R_p is particle radius (m), D_m is aqueous-phase diffusivity (m^2/s), and Sh, Re and Sc are Sherwood, Reynolds, and Schmidt dimensionless number, respectively. The intraparticle surface diffusion, D_s (m^2/s) is determined through empirical correlation by [47].

$$D_s = 8.6\times10^{-5}R_p\sqrt{\frac{D_m C_0}{Q_0}} \tag{7}$$

where C_0 is the inlet heavy metal ion concentration in fluid phase (mg/L) and Q_0 is the corresponding heavy metal ion concentration in solid phase (mg/g)

2.2.3. Adsorption isotherm model

The non-linear Langmuir and Freundlich model were expressed in Eqs. (8) and (9), respectively.

Langmuir model,

$$Q_e = \frac{Q_{max}K_L C_0}{1 + K_L C_0} \tag{8}$$

Fruendlich model,

$$Q_e = K_F C_0^{\frac{1}{n}} \tag{9}$$

The values of parameters Q_{max} and K_L for Langmuir model and K_F and $1/n$ for Freundlich model are stated in Section 2.1. The selection of isotherm models to be used in the simulation is according to the value of the coefficient determination, R^2. The higher R^2 close to unity indicates the model best described the experimental data. Therefore, for base-case simulation establishment, Fruendlich isotherm model is used.

2.3. Parametric studies

Parametric studies are performed to determine the effect of changing packed bed process parameters towards the adsorption performance, by evaluating the breakthrough curve profile. Four effects were evaluated, including inlet concentration, inlet flowrate, bed height and bed diameter. The parametric studies were conducted by changing around the original base value, as shown in Table 3.

Table 3. Parametric studies on the effect of four parameters, and the range of values used for this investigation.

Parameters	Range values studied
Inlet concentration, C_0 (mg/L)	10
	30
	50
Inlet flowrate, F ($\times 10^7$ m^3/s)	1.67
	2.00
	2.33
Bed height, H (cm)	20
	30
	40
Bed diameter, D (cm)	1.00
	1.43
	2.00

2.4. Upscale and sensitivity analysis

2.4.1. Industrial-scaled packed bed column

The Pb(II) ion adsorption onto activated alumina was scaled-up according to size of industrial wastewater application. A similar activated alumina column system of industrial-scaled was taken as reference for scaling up purpose [48]. The parameter's value of industrial-scaled bed column of the activated alumina system is presented in Table 4.

Table 4. Model parameter of activated alumina Plant D [48, 49].

Parameter	Value
Inlet flowrate, F (m^3/s)	6.31×10^{-4}
Hydraulic loading rate, v (m/s)	2.16×10^{-3}
Inlet concentration, C_o (mg/L)	0.1
Bed diameter, D (m)	0.6096
Bed height, H (m)	0.973
Residence time, τ (s)	450

The bed height was calculated using the residence time and hydraulic loading rate information, by using the relationship as expressed in Eq. (10) [50].

$$\tau = \frac{H}{v} \tag{10}$$

2.4.2. Sensitivity analysis

Sensitivity analysis was conducted on three parameters, namely the LDF mass transfer coefficient, bed porosity and isotherm model selection. This aimed to investigate the deviation they may cause if wrongly predicted or selected. Table 5 shows the range of values used for sensitivity analysis studies for the three parameters.

Table 5. The range used for sensitivity analysis investigation.

Parameter	Range
LDF mass transfer coefficient (1/s)	4.00×10^{-4} (five-fold increase) 8.00×10^{-5} (base value) 1.60×10^{-5} (five-fold decrease)
Bed porosity (m^3 void/m^3 bed)	0.32 (20% reduction) 0.40 (base value) 0.48 (20% increment)
Isotherm model	Langmuir ($R^2 = 0.974$) Freundlich ($R^2 = 0.994$)

3. Results and Discussion

3.1. Base simulation breakthrough curve establishment

A base simulation for the adsorption of Pb(II) onto activated alumina was established as a reference point, prior to the studies on the affecting parameters. The initial values specifications are presented in Table 6. The values in Table 6 will remain the same throughout the study except for the manipulated variable.

Table 6. Model parameters value used for base case simulation.

Parameter	Value
Inlet flowrate, F (m^3/s)	2×10^{-7}
Inlet concentration, C_o (mg/L)	30
Bed height, H (cm)	30
Bed diameter, D (cm)	1.43
Bed porosity, ε (m^3 void/m^3 bed)	0.4
Bulk density, ρ_s (kg/m^3)	810
External film mass transfer diffusion, k_f (m/s)	4.32791×10^{-5}
Intraparticle (surface) mass transfer diffusion, D_s (m^2/s)	2.7091×10^{-13}
Freundlich isotherm,	
K_F ([mg/g]/[mg/L]$^{1/n}$)	3.82
1/n	1.44

The plot of the base-case simulation breakthrough curve is shown in Fig. 1. The plot indicates that the column achieves breakthrough time at about 2.08 days, under the conditions stated in Table 6. The simulated breakthrough curve is consistent with other researchers as the shape is similar to an "S" shaped curve [51-54].

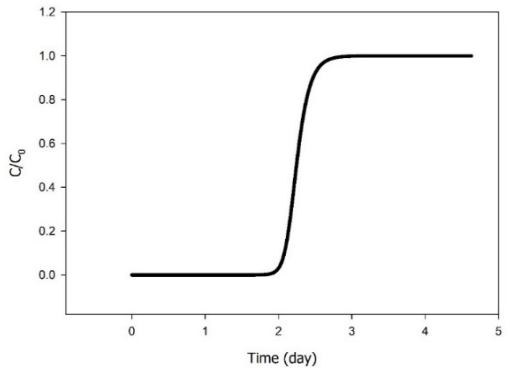

Fig. 1. Base simulation breakthrough curve.

For a better understanding of the Pb(II) adsorption process on activated alumina in a packed bed column, a concentration profile within the bed column is demonstrated in Fig. 2. When the bed column adsorption was conducted at 5,000, 50,000, 100,000, 150,000 and 400,000 seconds, the Pb(II) adsorbed into the bed column length of 0.04, 0.12, 0.20, 0.27 and 0.30 m, respectively. Additionally, the time to reach the saturation time at the packed bed column outlet was 2.88 days.

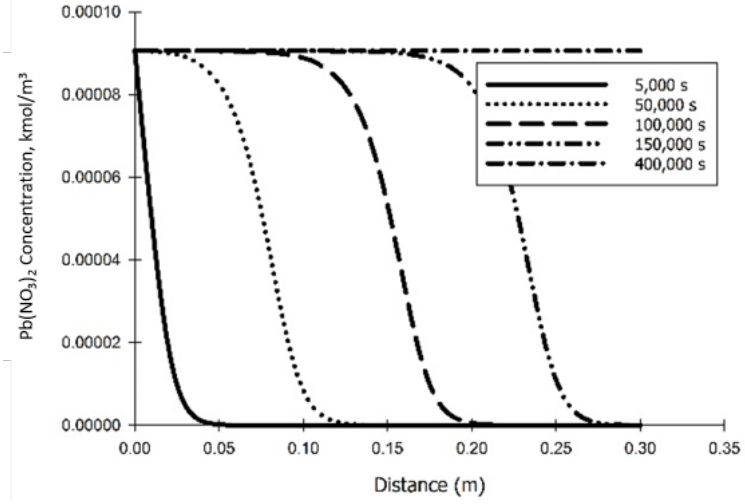

Fig. 2. Concentration profile of Pb(II) adsorption along the packed bed column filled with activated alumina.

3.2. Factors affecting breakthrough curve performance

The effects of various operating parameters, such as inlet flowrates, inlet metal ion concentrations, bed heights and bed diameters towards the dynamic packed bed column adsorption of Pb(II) onto activated alumina were studied and the breakthrough curves of plots of C/C_o versus time are presented in Figs. 3(a) to (d).

3.2.1. Effects of various inlet flowrates

The inlet Pb(II) flowrates of 1.67, 2.00 and 2.33 × 10^{-7} m^3/s were studied by fixing the values of inlet concentration, bed height and bed diameter at 30 mg/L, 30 cm, and 1.43 cm, respectively. As the inlet flowrates were increased from 1.67 to 2.33×10^{-7} m^3/s, the breakthrough curve achieves earlier breakthrough, as shown in Fig. 3(a). The break point time of the system decreases from 2.47 to 1.72 days.

This may due to an insufficient residence time between the Pb(II) ion and activated alumina, which led to a less physicochemical interactions between Pb(II) and activated alumina particles to achieve equilibrium at high flowrates [51, 55]. Subsequently, the solution may leave the column before adsorption equilibrium is achieved. A high flowrate also causes a chaotic turbulence phenomenon effect to occur along the bed, thus reducing the external mass transfer resistance [39].

3.2.2. Effects of various inlet metal ion concentrations

The inlet Pb(II) concentrations of 10, 30 and 50 mg/L were studied by fixing the values of inlet flowrate, bed height and diameter at 2.00×10-7 m^3/s, 30 cm, and 1.43 cm, respectively. It was observed that when the inlet Pb(II) concentrations were increased from 10 to 50 mg/L, the breakthrough time decreases, from 2.89 to 1.39 days as shown in Fig. 3(b).

A high Pb(II) concentration in the inlet feed causes the system to achieve an early breakthrough. This is because at a high Pb(II) concentration, the adsorption equilibrium may be attained faster due to an increase in the driving force of the concentration. Thus, more adsorbate being adsorbed and subsequently, shorten the breakthrough time and saturation time of the adsorbent [56].

It is also worth pointing out that by increasing the inlet concentration, the breakthrough curve is steepen, that may be due to the readily accessible of adsorption sites on the activated alumina to Pb(II) ions, in which were occupied instantaneously due to the diminished of mass transfer resistance at a higher inlet concentration [57].

3.2.3. Effect of various bed heights

The dynamic performance of the activated alumina in a packed bed column to remove Pb(II) were studied at 20, 30 and 40 cm, bed heights. The inlet flowrate, inlet concentration and bed diameter were fixed at 2×10^{-7} m^3/s, 30 mg/L and 1.43 cm, respectively.

As the bed heights were increased from 20 to 40 cm, the breakthrough time of the column was delayed, from 1.29 to 2.77 days as shown in Fig. 3(c). A longer bed, provides a larger surface area for a larger mass of Pb(II) [31, 55] to occupy the volume of a column leading to an increase in the breakthrough time.

In addition, the Pb(II) has more time to be in contact with the activated alumina particles at a longer bed height, therefore, caused a deep transport of Pb(II) molecules into the activated alumina, thus, results in a higher adsorption of Pb(II) ions [58].

3.2.4. Effect of various bed diameters

The effects of variation of the diameters of the bed towards the breakthrough curve were studied at 1.00, 1.43 and 2.00 cm. The inlet flowrate, inlet concentration and bed height were fixed at 2.00×10^{-7} m^3/s, 30 mg/L, and 30 cm, respectively.

As the bed diameters were increased from 1.00 to 2.00 cm, the breakthrough time increase from 0.90 to 4.16 days, as shown in Fig. 3(d). A column with a wider diameter, provides a larger cross-sectional area of active sites for the activated alumina adsorbent to occupy to promote sorption process [57].

In comparison, between bed height and bed diameter, varying the bed diameter give more pronounced changes on the breakthrough curves as shown in Figs. 3(c) and (d). This may be due to the increase of bed diameter, increases the cross-sectional area of the column, while increasing bed height only change the axial distance of the column. The data tabulated in Table 7 summarizes the discussion on the effect of parameters towards the dynamic column performance, in terms of breakthrough time.

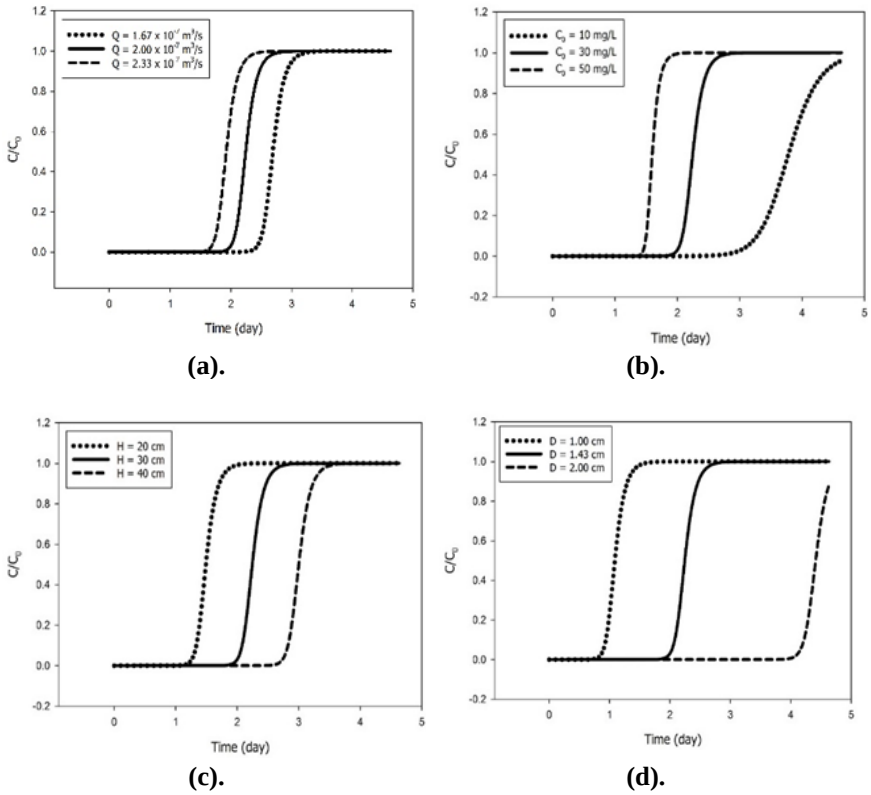

Fig. 3. Effect of (a) inlet flow rate [C0=30 mg/L, H=30 cm, D=1.43 cm]; (b) inlet concentration [F=2×10-7 m^3/s, H=30 cm, D=1.43 cm]; (c) bed height [F=2×10-7 m^3/s, C0=30 mg/L, D=1.43 cm]; (d) bed diameter [F=2×10-7 m^3/s, C0=30 mg/L, H=30 cm] on the breakthrough curve.

Table 7. Summary of activated alumina breakthrough time under various operating conditions.

Run no.	Inlet flowrate (×10^7 m^3/s)	Inlet concentration (mg/L)	Bed height (cm)	Bed diameter (cm)	Breakthrough time (days)
1	1.67	30	30	1.43	2.47
2	2.00	30	30	1.43	2.03
3	2.33	30	30	1.43	1.72
4	2.00	10	30	1.43	2.89
5	2.00	50	30	1.43	1.39
6	2.00	30	20	1.43	1.29
7	2.00	30	40	1.43	2.77
8	2.00	30	30	1.00	0.90
9	2.00	30	30	2.00	4.16

3.3. Upscale and sensitivity analysis

An industrial-scaled packed column of Plant D was employed for upscaling purposes. The base case of the simulation in Section 3.1 was scaled-up according to the design specification of Plant D as stated in Table 4. The scaled-up packed system was able to achieve a breakthrough time of 17 days, based on the breakthrough curve shown in Fig. 4.

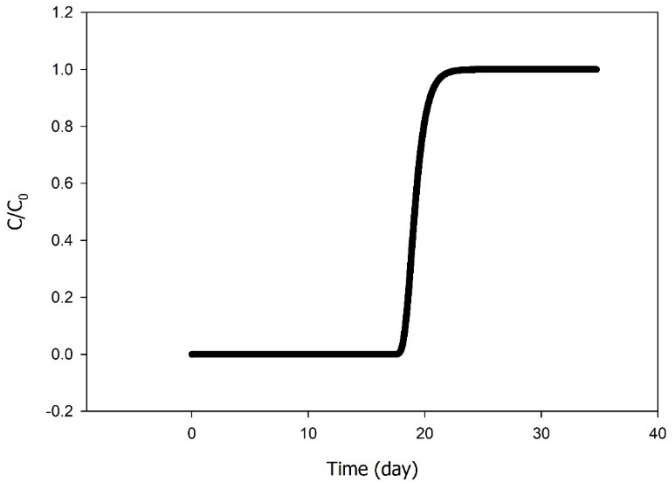

Fig. 4. Up-scaled breakthrough curve.

3.3.1. Influence of LDF mass transfer coefficient

The influence of variation of the overall mass transfer coefficient on the breakthrough time of the system was investigated. It shows that the overall mass transfer coefficient, combining both external film and intraparticle surface diffusion improves the mass transfer at high MTC as shown in Fig. 5(a).

The breakthrough curve of the activated alumina system was not greatly influenced by the changes in the overall mass transfer coefficient. It is obvious that with the parameter values used, it is more notable at lower values of MTC.

The influence of reduction by five-folds from the base value of MTC = 8×10^{-5} 1/s is much more significant than that for a five-folds increase in the MTC. A slow approach of C/C_0 toward 1 was observed at lower MTC, which most probably due to the slow intraparticle surface diffusion within the pores of activated alumina particles [52]. Bono (1989) also reaches the similar finding [45]. The mass transfer correlations from literature are usually subject to about 20% error [59]. This analysis confirmed that for the system at hand, such LDF mass transfer uncertainty is unlikely to influence the activated alumina dynamic column performance.

3.3.2. Influence of bed porosity

The influence of bed porosity on the breakthrough time was plotted as shown in Fig. 5(b). The plot in Fig. 5(b) suggests that the influence of ±20% of bed porosity is significant to an activated alumina system.

One possible reason for this phenomenon is that a lower bed porosity results in higher residence time of the adsorbate in the bed column due to more tortuous path of the adsorbate molecules [60]. Thus, the adsorption effects are significantly diminished at higher porosity.

3.3.3. Influence of isotherm model

The influence of different isotherm models on the breakthrough curve of up-scaled system was investigated. The plot of C/C_o against time is shown in Fig. 5(c). The parameter value of inlet flowrate, inlet concentration, bed height and bed diameter are presented in Table 4.

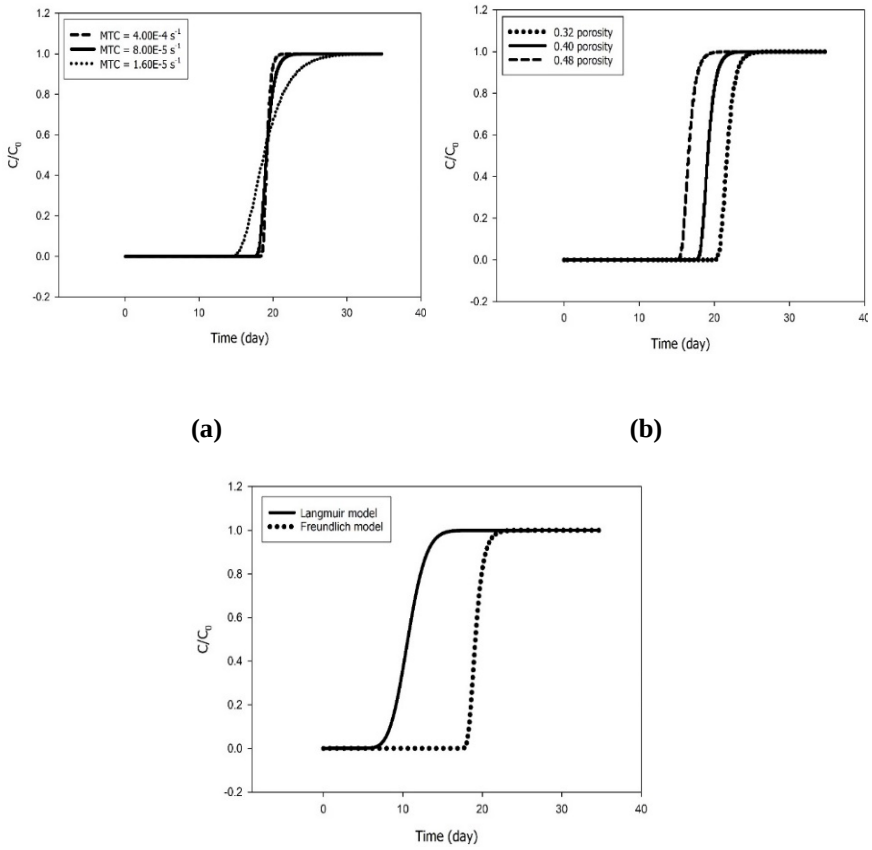

Fig. 5. Influence of (a) MTC; (b) bed porosity; (c) isotherm model on breakthrough curve of Pb(II) onto activated alumina.

Based on Fig. 5(c), the Freundlich isotherm model shows a latter breakthrough time compared to the Langmuir isotherm model. This situation gives insight that the wrong selection of isotherm model could greatly affect the results of breakthrough curve performance of a system, with over 50% difference. Hence, the

selection of a right isotherm model is crucial and need to be evaluated carefully to give appropriate results.

3.3.4. Industrial application

The residence time of the bed column was increased one-half- and two-folds from the original residence time of 450 s. Table 8 shows the specification for simulation of three different residence time (or bed height).

The breakthrough time of the system at different residence time was plotted on the same graph as shown in Fig. 6, to investigate the possible height of bed column that was considered feasible for industrial application in terms of manageability and personnel operability.

Table 8. Model parameters of several bed heights for industrial application.

Parameter	Value
Inlet flowrate, F (m^3/s)	6.31×10^{-4}
Hydraulic loading rate, v (m/s)	2.16×10^{-3}
Inlet concentration, C_o (mg/L)	0.1
Bed diameter, D (m)	0.6096
Bed height, H (m)	0.973, 1.459, 1.946
Residence time, τ (s)	450, 675, 900

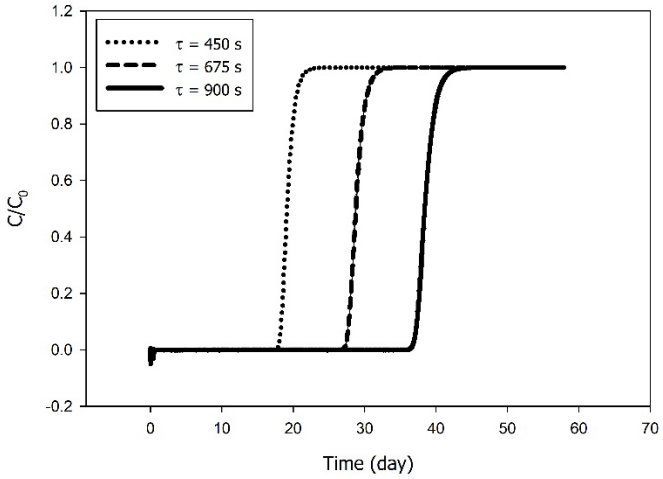

Fig. 6. Packed bed column at different residence time (or bed height).

It is shown that the residence time of 450 to 900 secs seems to be a conservative value of activated alumina plant design as at this residence time range, the bed height of the column is considered manageable and easy for operation as well as personnel operability for media replacement. When the residence time of the column increases from 450 to 900 sec, the breakthrough time of the column increased from about 17.36 to 37.04 days. Increase in residence time indicates that the solute adsorbate has more time in the bed column, which means that when the residence time is increased, the height of the bed column in also increased.

Of three different residence time or bed height, the residence time of 675 secs or the equivalent bed height of 1.459 m seems to be practical and manageable for industrial used in wastewater treatment of industrial effluent as the breakthrough time is 28 days.

The breakthrough time of industrial-sized activated alumina packed bed column for the removal of Pb(II) has been compared with other industrial-sized packed bed column of other systems reported in the literature and the values have been summarized in Table 9. The values and comparisons reported have only a relative meaning because each study was conducted under different conditions such as inlet flow rate, inlet concentration, bed height, bed diameter, as well as the type of adsorbent materials that contributes to different adsorption capacity for each adsorbate. The study of present investigation shows that activated alumina in packed bed column of industrial sized exhibit a reasonable breakthrough time in removing Pb(II) from aqueous solutions.

Table 9. Comparison of results with literature.

Parameter	**Pb(II)**	**Pb(II)**	**Tetrachloro ethene**	**Trichloro ethene**	**Pb(II)**
Adsorbent	Olive tree pruning biosorbent	Olive tree pruning biosorbent	Granular activated carbon	Granular activated carbon	Activated alumina
Bed diameter, D (m)	0.50	0.50	2.44	2.44	0.6096
Bed height, H (m)	2.26	3.77	0.417	0.417	1.459
Initial concentration, C_0 (mg/L)	100	100	2.281	3.397	0.1
Flow rate, F (m^3/s)	1.482×10^{-3}	2.469×10^{-3}	6.483×10^{-3}	6.483×10^{-3}	6.310×10^{-4}
Breakthrough time, t_b (days)	0.14	0.21	451	122	28
Reference	[39]	[39]	[61]	[61]	This study

4. Conclusion

In this study, the simulation of dynamic adsorption of lead (II) ions onto activated alumina in a packed bed column was investigated. With appropriate isotherm model selection and reliable prediction of MTC, activated alumina packed bed column for removing Pb(II) can be modelled and solved by available simulation package. The effect of inlet flowrate, inlet concentration, bed height and bed diameter towards the performance of the system were examined by varying one parameter at a time, while the others were kept constant. The sensitivity analysis was conducted to check whether the presumed or predicted parameters could deviate much the results if wrongly selected or predicted. A packed bed column of industrial-scaled dimensions and operational settings were selected for evaluation of the lead (II)-activated alumina system for industrial application in wastewater treatment.

Based on this present study, some conclusions could be drawn. First, the inlet flowrate and inlet concentration are inversely proportional to the breakthrough time of the system. While the bed height and bed diameter are directly proportional to

the breakthrough time of the system. Bed diameter effect on the system's performance is more significant than bed height as it involves the alteration of the column cross-sectional area. In addition, the sensitivity analysis indicates that the wrong selection of isotherm model in the simulation could deviate the results up to 50%, while the changes of the LDF mass transfer coefficient is not greatly influence the system' performance.

The industrial-scaled packed bed column with height of 1.459 m and diameter of 0.6096 m is chosen, with the column operation time of 28 days, to be an applicable and manageable size for industrial application in wastewater treatment. However, some further works need to be executed to establish and verify the applicability of this simulation study for further design consideration, for instance continuous multistage series adsorption.

Acknowledgment

The authors acknowledge the financial support given by the Ministry of Higher Education for this study under the Fundamental Research Grant Scheme (FRGS) number FRG0511-1/2019.

Nomenclatures

A	Cross-sectional area of the column, m^2
C	Aqueous-phase concentration, mg/L
D	Bed column diameter, m
D_L	Axial dispersion coefficient, m^2/s
D_m	Molecular diffusivity, m^2/s
D_s	Intraparticle surface mass transfer diffusion, m^2/s
F	Inlet flowrate, m^3/s
H	Bed column height, m
i	Component i
k_f	External film mass transfer diffusion, m/s
K_F	Freundlich adsorption capacity, $(mg/g)/(mg/L)^{1/n}$
K_L	Langmuir adsorption affinity, L/mg
M	Molecular weight of solute, kg/kmol
MTC	LDF mass transfer coefficient, 1/s
$1/n$	Freundlich adsorption affinity
0	Initial state
Q	Solid-phase loading, mg/g
Q_{max}	Maximum adsorption capacity, mg/g
R_p	Particle radius, m
Re	Reynolds number
Sc	Schmidt number
Sh	Sherwood number
T	Temperature, °C
V_s	Volume of solid, m^3
z	Bed axial position, m

Greek Symbols

ε	Bed porosity, m^3 void/m^3 bed
ρ_s	Bulk solid density, kg/m^3

τ	Residence time, s
u_o	Fluid interstitial velocity, m/s
v	Hydraulic loading rate, m/s

References

1. Castro, L.; Blázquez, M.L.; González, F.; Muñoz, J.A.; and Ballester, A. (2017). Biosorption of Zn(II) from industrial effluents using sugar beet pulp and *F. vesiculosus*: from laboratory tests to a pilot approach. *Science of The Total Environment*, 598, 856-866.
2. Wani, A.L.; Ara, A.; and Usmani, J.A. (2015). Lead toxicity: a review. *Interdisciplinary Toxicology*, 8(2), 55-64.
3. Awual, M.R.; Hasan, M.M.; Islam, A.; Rahman, M.M.; Asiri, A.M.; Khaleque, M.A.; and Sheikh, M.C. (2019). Offering an innovative composited material for effective lead(II) monitoring and removal from polluted water. *Journal of Cleaner Production*, 231, 214-223.
4. Mohammadi, S.; Mehrparvar, A.H.; and Aghilinejad, M. (2008). Appendectomy due to lead poisoning: a case-report. *Journal of Occupational Medicine and Toxicology*, 3.
5. Karrari, P.; Mehrpour, O.; and Abdollahi, M. (2012). A systematic review on status of lead pollution and toxicity in Iran; guidance for preventive measures. *DARU Journal of Pharmaceutical Sciences*, 20(1), 1-17.
6. Jan, A.T.; Azam, M.; Siddiqui, K.; Ali, A.; Choi, I.; and Haq, Q.M.R. (2015). Heavy metals and human health: mechanistic insight into toxicity and counter defense system of antioxidants. *International Journal of Molecular Sciences*, 16(12), 29592-29630.
7. Calero, M.; Hernáinz, F.; Blázquez, G.; Tenorio, G.; and Martín-Lara, M.A. (2009). Study of Cr (III) biosorption in a fixed-bed column. *Journal of Hazardous Materials*, 171(1-3), 886-893.
8. Assi, M.A.; Hezmee, M.N.M.; Haron, A.W.; Sabri, M.Y.M.; and Rajion, M.A. (2016). The detrimental effects of lead on human and animal health. *Veterinary World*, 9(6), 660-671.
9. Yao, Z.Y.; Qi, J.H.; and Wang, L.H. (2010). Equilibrium, kinetic and thermodynamic studies on the biosorption of Cu (II) onto chestnut shell. *Journal of Hazardous Materials*, 174, 137-143.
10. Sud, D.; Mahajan, G.; and Kaur, M.P. (2008). Agricultural waste material as potential adsorbent for sequestering heavy metal ions from aqueous solutions – a review. *Bioresource Technology*, 99(14), 6017-6027.
11. Zhang, L.; Zhao, L.; Yu, Y.; and Chen, C. (1998). Removal of lead from aqueous solution by non-living *rhizopus nigricans*. *Water Research*, 32(5), 1437-1444.
12. Caetano, A.; Pinho, M.N.; Drioli, E.; and Muntau, H. (1995). *Membrane technology: applications to industrial wastewater treatment* (1st ed.). Amsterdam: Springer Netherlands.
13. Xiu, G.; and Li, P. (2000). Prediction of breakthrough curves for adsorption of lead (II) on activated carbon fibers in a fixed bed. *Carbon*, 38(7), 975-981.

14. Tien, C. (2018). *Introduction to adsorption: basics, analysis, and applications* (1st ed.). Amsterdam: Elsevier.
15. Boudrahem, F.; Aissani-Benissad, F.; and Soualah, A. (2011). Adsorption of lead(II) from aqueous solution by using leaves of date trees as an adsorbent. *Journal of Chemical and Engineering Data*, 56(5), 1804-1812.
16. Awual, M.R. (2019). Efficient phosphate removal from water for controlling eutrophication using novel composite adsorbent. *Journal of Cleaner Production*, 228, 1311-1319.
17. Awual, M.R. (2019). Novel ligand functionalized composite material for efficient copper(II) capturing from wastewater sample. *Composites Part B: Engineering*, 172, 387-396.
18. Ronda, A.; Martín-Lara, M.A.; Dionisio, E.; Blázquez, G.; and Calero, M. (2013). Effect of lead in biosorption of copper by almond shell. *Journal of the Taiwan Institute of Chemical Engineers*, 44(3), 466-473.
19. Barquilha, C.E.R.; Cossich, E.S.; Tavares, C.R.G.; and Silva, E.A. (2017). Biosorption of nickel(II) and copper(II) ions in batch and fixed-bed columns by free and immobilized marine algae *Sargassum* sp. *Journal of Cleaner Production*, 150, 58-64.
20. Prasad, M.; Saxena, S.; Amritphale, S.S.; and Chandra, N. (2000). Kinetics and isotherms for aqueous lead adsorption by natural minerals. *Industrial and Engineering Chemistry Research*, 39(8), 3034-3037.
21. Du, C.; Liu, H.; Xiao, M.; Gao, D.; Huang, D.; Li, Z.; Chen, T.; Mo, J.; Wang, K.; and Zhang, C. (2012). Adsorption of iron and lead ions from an aqueous solution by plasma-modified activated carbon. *Industrial and Engineering Chemistry Research*, 51(48), 15618-15625.
22. Naiya, T.K.; Bhattacharya, A.K.; and Das, S.K. (2009). Adsorption of Cd(II) and Pb(II) from aqueous solutions on activated alumina. *Journal of Colloid and Interface Science*, 333, 14-26.
23. Bhat, A.; Megeri, G.B.; Thomas, C.; Bhargava, H.; Jeevitha, C.; Chandrashekar, S.; and Madhu, G.M. (2015). Adsorption and optimization studies of lead from aqueous solution using γ-Alumina. *Journal of Environmental Chemical Engineering*, 3(1), 30-39.
24. Mohammad, N.K.; Ghaemi, A.; and Tahvildari, K. (2019). Hydroxide modified activated alumina as an adsorbent for CO_2 adsorption: experimental and modeling. *International Journal of Greenhouse Gas Control*, 88, 24-37.
25. Das, N.; Vimala, R.; and Karthika, P. (2008). Biosorption of heavy metals - an overview. *Indian Journal of Biotechnology*, 7, 159-169.
26. Anisuzzaman, S.M.; Bono, A.; Krishnaiah, D.; and Tan, Y.Z. (2016). A study on dynamic simulation of phenol adsorption in activated carbon packed bed column. *Journal of King Saud University - Engineering Sciences*, 28(1), 47-55.
27. Girish, C.R.; and Ramachandra, M.V. (2013). Removal of phenol from wastewater in packed bed and fluidised bed columns: a review. *International Research Journal of Environment Sciences*, 2(10), 96-100.
28. Ye, J.; Hu, A.; Ren, G.; Chen, M.; Tang, J.; Zhang, P.; Zhou, S.; and He, Z. (2018). Enhancing sludge methanogenesis with improved redox activity of extracellular polymeric substances by hematite in red mud. *Water Research*, 134, 54-62.

29. Hu, A.; Ren, G.; Che, J.; Guo, Y.; Ye, J.; and Zhou, S. (2020). Phosphate recovery with granular acid-activated neutralized red mud: fixed-bed column performance and breakthrough curve modelling. *Journal of Environmental Sciences*, 90, 78-86.
30. Hanafy, H.; Sellaoui, L.; Thue, P.S.; Lima, E.C.; Dotto, G.L.; Alharbi, T.; Belmabrouk, H.; Bonilla-Petriciolet, A.; and Lamine, A.B. (2020). Statistical physics modeling and interpretation of the adsorption of dye remazol black B on natural and carbonized biomasses. *Journal of Molecular Liquids*, 299.
31. Yanyan, L.; Kurniawan, T.A.; Zhu, M.; Ouyang, T.; Avtar, R.; Othman, M.H.D.; Mohammad, B.T.; and Albadarin, A.B. (2018). Removal of acetaminophen from synthetic wastewater in a fixed-bed column adsorption using low-cost coconut shell waste pretreated with NaOH, HNO_3, ozone, and/or chitosan. *Journal of Environmental Management*, 226, 365-376.
32. Lu, P.J.; Chang, C.S.; and Chern, J.M. (2014). Binary adsorption breakthrough curves in fixed bed: experiment and prediction. *Journal of the Taiwan Institute of Chemical Engineers*, 45(4), 1608-1617.
33. Hodaifa, G.; Alami, S.B.D.; Ochando-Pulido, J.M.; and Víctor-Ortega, M.D. (2014). Iron removal from liquid effluents by olive stones on adsorption column: breakthrough curves. *Ecological Engineering*, 73, 270–275.
34. Long, Y.; Jiang, J.; Hu, J.; Hu, X.; Yang, Q.; and Zhou, S. (2019). Removal of Pb(Ⅱ) from aqueous solution by hydroxyapatite/carbon composite: preparation and adsorption behavior. *Colloids and Surfaces A: Physicochemical and Engineering Aspects*, 577, 471-479.
35. Pam, A.A.; Abdullah, A.H.; Tan, Y.P.; and Zainal, Z. (2018). Batch and fixed bed adsorption of Pb(II) from aqueous solution using EDTA modified activated carbon derived from palm kernel shell. *BioResources*, 13(1), 1235-1250.
36. Upadhyay, R.; Pandey, P.K.; and Pardeep. (2017). Adsorption of Cu(II) and Cr(VI) by zeolite in batch and column mode. *Materials Today: Proceedings*, 4(9), 10504-10508.
37. Turan, M.; Mart, U.; Yüksel, B.; and Çelik, M.S. (2005). Lead removal in fixed-bed columns by zeolite and sepiolite. *Chemosphere*, 60, 1487-1492.
38. Kopsidas, O.N.; Konstantinou, I.G.; Sidiras, D.K.; and Batzias, F.A. (2019). Scale up of adsorption column packed with conditioned waste lignocellulosics. *Proceedings of the International Conference of Computational Methods in Sciences and Engineering*. Rhodes, Greece.
39. Ronda, A.; Martin-Lara, M.A.; Osegueda, O.; Castillo, V.; and Blázquez, G. (2018). Scale-up of a packed bed column for wastewater treatment. *Water Science and Technology*, 77(5-6), 1386-1396.
40. Hu, Q.; Xie, Y.; and Zhang, Z. (2020). Modification of breakthrough models in a continuous-flow fixed-bed column: mathematical characteristics of breakthrough curves and rate profiles. *Separation and Purification Technology*, 238.
41. Bonilla-Petriciolet, A.; Mendoza-Castillo, D.I.; Dotto, G.L.; and Duran-Valle, C.J. (2019). Adsorption in water treatment. *Reference Module in Chemistry, Molecular Sciences and Chemical Engineering*.

42. Glueckauf, E. (1955). Theory of chromatography. Part 10-formulae for diffusion into spheres and their application to chromatography. *Transactions of the Faraday Society*, 51, 1540-1551.
43. AspenONE (2009). *AspenONE v7.3 Reference guide*. United States: Aspen Technology Inc.
44. Knox, J.C.; Ebner, A.D.; Levan, M.D.; Coker, R.F.; and Ritter, J.A. (2016). Limitations of breakthrough curve analysis in fixed-bed adsorption. *Industrial and Engineering Chemistry Research*, 55(16), 4734-4748.
45. Bono, A. (1989). *Sorptive separation of simple water soluble organics*. PhD thesis. England: University of Surrey.
46. Ohashi, H.; Sugawara, T.; Kikuchi, K.; and Konno, H. (1981). Correlation of liquid-side mass transfer coefficient for single particles and fixed beds. *Journal of Chemical Engineering of Japan*, 14(6), 433-438.
47. Worch, E. (2008). Fixed-bed adsorption in drinking water treatment : a critical review on models and parameter estimation. *Journal of Water Supply: Research and Technology - Aqua*, 57(3), 171-183.
48. Wang, L.; Chen, A.; and Fields, K. (2000). *Arsenic removal from drinking water by ion exchange and activated alumina plants*. Ohio: National Service Center for Environmental Publications.
49. Bhardwaj, V.; Kumar, P.; and Singhal, G. (2014). Toxicity of heavy metals pollutants in textile mills effluents. *International Journal of Scientific and Engineering Research*, 5(7), 664-666.
50. Worch, E. (2012). *Adsorption technology in water treatment: fundamentals, processes, and modelling* (1st ed.). Berlin: Walter de Gruyter.
51. Babu, B.V; and Gupta, S. (2006). Modeling and simulation of fixed bed adsorption column: effect of velocity variation. *Journal on Future Engineering and Technology*, 1(1), 60-66.
52. Lin, X.; Huang, Q.; Qi, G.; Shi, S.; Xiong, L.; Huang, C.; Chen, X.; Li, H.; and Chen, X. (2017). Estimation of fixed-bed column parameters and mathematical modeling of breakthrough behaviors for adsorption of levulinic acid from aqueous solution using SY-01 resin. *Separation and Purification Technology*, 174, 222-231.
53. Sperlich, A.; Schimmelpfennig, S.; Baumgarten, B.; Genz, A.; Amy, G.; Worch, E.; and Jekel, M. (2008). Predicting anion breakthrough in granular ferric hydroxide (GFH) adsorption filters. *Water Research*, 42(8-9), 2073-2082.
54. Vera, L.M.; Bermejo, D.; Uguña, M.F.; Garcia, N.; Flores, M.; and González, E. (2019). Fixed bed column modeling of lead (II) and cadmium (II) ions biosorption on sugarcane bagasse. *Environmental Engineering Research*, 24(1), 31-37.
55. Banerjee, M.; Basu, R.K.; and Das, S.K. (2019). Adsorptive removal of Cu(II) by pistachio shell: Isotherm study, kinetic modelling and scale-up designing — continuous mode. *Environmental Technology and Innovation*, 15.
56. Xu, S.; Liang, M.; Zhang, L.; Tang, S.; Zhu, Z.; and Zhu, L. (2019). Packed bed column investigation on As(V) adsorption using magnetic iron oxide/bagasse biomass carbon composite adsorbent. *IOP Conference Series: Materials Science and Engineering*, 490(3).

57. Meshram, P.D.; and Bhagwat, S.S. (2020). Dynamic adsorption of Cd^{2+} from aqueous solution using biochar of pine-fruit residue. *Indian Chemical Engineer*, 62(2), 170-183.
58. Ahmed, M.J.; and Hameed, B.H. (2018). Removal of emerging pharmaceutical contaminants by adsorption in a fixed-bed column: A review. *Ecotoxicology and Environmental Safety*, 149, 257-266.
59. Kataoka, T.; Yoshida, H.; and Ueyama, K. (1972). Mass transfer in laminar region between liquid and packing material surface in the packed bed. *Journal of Chemical Engineering of Japan*, 5(2), 132-136.
60. Basu, A.; Mustafiz, S.; Islam, M.R.; Bjorndalen, N.; Rahaman, M.S.; and Chaalal, O. (2006). A comprehensive approach for modeling sorption of lead and cobalt ions through fish scales as an adsorbent. *Chemical Engineering Communications*, 193(5), 580-605.
61. Crittenden, J.; Berrigan, J.D.; Hand, D.; and Friedman, G. (1986). *Scale-up of rapid small-scale adsorption tests to field-scale adsorbers: theoretical basis and experimental results for a constant diffusivity*. Washington DC: U.S. Environmental Protection Agency.